Action Potential Propagation in Myelinated Nerve Fibers

Gautam K. Luhana, Richard Xu

May 2018

1 Introduction

Hodgkin and Huxley's model for voltage propagation in the squid giant axon was based off experimental data taken from an unmyelinated nerve fiber (Hodgkin and Huxley, 1952). Because unmyelinated axons are typically only found in invertebrates, we are interested in the behavior of myelinated axons. We extend the Hodgkin and Huxley equations to simulate the behavior of a myelinated nerve fiber with multiple Nodes of Ranvier and internodal sections.

Myelin is a layer of electrically insulating material that surrounds the axons of many nerve cells. The myelinated sections of an axon typically have a length of 2 millimeters and are separated by unmyelinated sections called Nodes of Ranvier which typically have a length of 2 micrometers. Thus, the myelinated sections are generally on the order of 1000 times longer than the unmyelinated sections. The purpose of the myelin on the internodal sections is to increase the speed of voltage propagation through the axon. Experimental results have shown that voltage can propagate through a myelinated axon at speeds up to 200 m/s while voltage moves through an unmyelinated axon at a speed of only 2 m/s. Because the myelinated sections of the cable do not have voltage-gated ion channels, we say that those sections are "passive" cables as opposed to the Nodes of Ranvier, which we call "active" cables.

2 Myelinated vs Unmyelinated Axons

In creating a model analogous to the Hodgkin-Huxley equations, there are several differences between myelinated and unmyelinated axons that need to be considered.

1. Although the length of the passive cable can be over 1000 times longer than the active cable, its total capacitance is around the same as that of the active cable. Thus, the capacitance of the myelinated cable per unit area needs to be several orders of magnitude smaller.
2. The myelin is a layer of lipids that wrap around the axon up to several hundred times, preventing the leak of ions through the membrane of the axon. Thus, the resistance of the membrane of the passive cable is also several orders of magnitude higher than the resistance of the unmyelinated membrane. This corresponds to a much lower leakage constant in the original Hodgkin-Huxley equation.
3. Because the myelin layer is quite thick, the radius of the myelinated section is around 1.5 times larger than the radius of the unmyelinated cable.
4. The myelin layer prevents the active pumping of sodium and potassium ions in the passive cable.
5. The density of sodium ion channels in the Nodes of Ranvier of a myelinated cable is much higher than that of the unmyelinated cable because a stronger action potential needs to be generated in order for it to propagate through the passive sections.

6. The giant axon of the squid is unmyelinated so the parameters of the Hodgkin-Huxley model, especially the length and diameter of the cable, may not facilitate successful action potential propagation through myelinated sections

7. The junctions between the active and passive cables need special treatment to maintain numerical accuracy because the two cables have very differerent properties

8. Unmyelinated axons experience something called hyperpolarization during which the voltage of a cable goes below its rest potential of -70 mV. Myelinated axons do not hyperpolarize because it would also cause the hyperpolarization of the passive cables. This would make it difficult for later action potentials to propagate through the cable due to the low resistance of the passive sections.

3 Equations

Listed below are the equations used for modeling both the active and passive sections of the cable. Rather than taking the rest potential to be 0, we shifted the voltage so that the rest potential is at -70 mV which more accurately represents the true rest voltage of an unmyelinated cable. We simulated both an unmyelenated and myelenated cable of approximately the same length to check voltage propagation speeds. In the unmyelenated cable, only the parameters and equations of the active sections were considered with their usual values in the Hodgkin Huxley system of equations.

$$C_A \frac{\partial V}{\partial t} = \frac{r_A}{2\rho_A} \frac{\partial^2 V}{\partial x^2} - g(V - E) \tag{1}$$

$$C_P \frac{\partial V}{\partial t} = \frac{r_P}{2\rho_P} \frac{\partial^2 V}{\partial x^2} - \overline{g_{LP}}(V - E_{LP}) \tag{2}$$

$$\frac{dm}{dt} = \alpha_m(V)(1 - m) - \beta_m(V)m \tag{3}$$

$$\frac{dn}{dt} = \alpha_n(V)(1 - n) - \beta_n(V)n \tag{4}$$

$$\frac{dh}{dt} = \alpha_h(V)(1 - h) - \beta_h(V)h \tag{5}$$

$$i(t) = -\frac{\pi r_A^2}{\rho_A} \frac{\partial V(0,t)}{\partial x} \tag{6}$$

$$0 = -\frac{\pi r_A^2}{\rho_A} \frac{\partial V_A}{\partial x} - \frac{\pi r_P^2}{\rho_P} \frac{\partial V_P}{\partial x} \tag{7}$$

$$0 = -\frac{\pi r_A^2}{\rho_A} \frac{\partial V(L,t)}{\partial x} \tag{8}$$

$$g = \overline{g_{Na}} m^3 h(V - E_{Na}) + \overline{g_K} n^4 (V - E_K) + \overline{g_L}(V - E_{LA}) \tag{9}$$

$$E = \frac{1}{g}\left(\overline{g_{Na}} E_{Na} m^3 h(V - E_{Na}) + \overline{g_K} E_K n^4 (V - E_K) + \overline{g_L} E_L (V - E_{LA})\right) \tag{10}$$

$$i(t) = \begin{cases} i_0 & \text{if } t_1 \le t \le t_2 \\ 0 & \text{otherwise} \end{cases} \tag{11}$$

where the $\alpha(V)$ and $\beta(V)$ functions are

$$\alpha_m(V) = \frac{\frac{V+45}{10}}{1 - e^{-\frac{V+45}{10}}}$$
$$\beta_m(V) = 4e^{-\frac{V+70}{18}}$$
$$\alpha_n(V) = 0.1\frac{\frac{V+60}{10}}{1 - e^{-\frac{V+60}{10}}}$$
$$\beta_n(V) = 0.125e^{-\frac{V+70}{80}}$$
$$\alpha_h(V) = 0.07e^{-\frac{V+70}{20}}$$
$$\beta_h(V) = \frac{1}{1 + e^{-\frac{V+40}{10}}}$$

The parameters, their associated meanings and values are listed below

$V(x,t) =$ voltage (mV)
$t =$ time $(msec)$
$x =$ distance along the axon (cm)

$m(x,t) =$ dimensionless sodium activation variable
$n(x,t) =$ dimensionless potassium activation variable
$h(x,t) =$ dimensionless sodium inactivation variable
$C_A =$ capacitance per unit area of the active cable $= 1.0$ $(\mu F/cm^2)$
$C_P =$ capacitance per unit area of the passive cable $= 0.004$ $(\mu F/cm^2)$
$r_A =$ radius of the active cable $= 0.005$ (cm)
$r_P =$ radius of the passive cable $= 0.007$ (cm)
$\rho_A =$ axoplasmic resistivity of the active cable $= 0.0354$ $(k\Omega\ cm)$
$\rho_P =$ axoplasmic resistivity of the passive cable $= 0.0354$ $(k\Omega\ cm)$
$\overline{g_{Na}} =$ membrane sodium conductance per unit area in the active cable $= 2400$ $(k\Omega/cm^2)$
$\overline{g_K} =$ membrane potassium conductance per unit area in the active cable $= 400$ $(k\Omega/cm^2)$
$\overline{g_{LA}} =$ membrane leakage per unit area in the active cable $= 0.3$ $(k\Omega/cm^2)$
$\overline{g_{LP}} =$ membrane leakage per unit area in the passive cable $= 0.0012$ $(k\Omega/cm^2)$
$E_{Na} =$ membrane reversal potential for sodium $= 45$ (mV)
$E_K =$ membrane reversal potential for potassium $= -83$ (mV)
$E_{LA} =$ membrane leakage reversal potential in the active cable $= -59$ (mV)
$E_{LP} =$ membrane leakage reversal potential in the passive cable $= -70$ (mV)
$V_A =$ voltage at an active cable point next to a junction (mV)
$V_P =$ voltage at a passive cable point next to a junction (mV)
$L =$ length of the cable (cm)
$i(t) =$ stimulating current as a function of time $(\mu A/m)$
$i_0 =$ constant value of current between t_1 and t_2 $= 30$ $(\mu A/m)$
$t_1 =$ start time of stimulating current $= 0.01$ $(msec)$
$t_2 =$ end time of stimulating current $= 0.02$ $(msec)$

Equation (1) is the classical Hodgkin-Huxley equation, except $\overline{g_{Na}}$ is 20 times higher in this equation and $\overline{g_K}$ is approximately 10 times higher. Equation (2) is a linear cable equation that describes the behavior of the passive cable. The capacitance of the passive cable, C_P is 250 times smaller than the capacitance of the active cable, C_A. Equation (6) describes the boundary condition at the start of the cable where a stimulating current is injected into the axon. Equation (7) describes the boundary conditions at the junctions of the passive and active cables and Equation (8) describes the boundary condition at the end of the cable. These boundaries are derived from the fact that the sum of the currents at these points must be equal to 0 or in the case of the state node, $i(t)$.

4 Numerical Method

We discretize our voltage and our gating variables with the following indices

$$V_j^k = V(j\Delta x, k\Delta t) \tag{12}$$

$$s_j^{k+1/2} = s(j\Delta x, (k+1/2)\Delta t) \tag{13}$$

where s represents any one of the gating variables (n, m or h) and j ranges from 0 to $n-1$

We time step our gating variable using the formula

$$\frac{s_j^{k+1/2} - s_j^{k-1/2}}{\Delta t} = \alpha_s(V_j^k)\left(1 - \frac{s_j^{k+1/2} + s_j^{k-1/2}}{2}\right) - \beta_s(V_j^k)\left(\frac{s_j^{k+1/2} + s_j^{k-1/2}}{2}\right) \tag{14}$$

The gating variables are evaluated in half intervals between each V^k evaluation and instead of using just $s_j^{k-1/2}$ to evaluate the next time step, $s_j^{k+1/2}$, an average is taken between the two values to create an implicit formula for $s_j^{k+1/2}$. However, this can be made explicit for $s_j^{k+1/2}$ in terms of $s_j^{k-1/2}$ and V_j^k

The voltage is evaluated using the following formulas

$$C_A\frac{V_j^{k+1} - V_j^k}{\Delta t} = -g_j^{k+1/2}\left(\frac{V_j^{k+1} + V_j^k}{2} - E_j^{k+1/2}\right) + \frac{r_A}{2\rho_A}\left(D^+D^-\frac{V^{k+1} + V^k}{2}\right)_j \tag{15}$$

$$C_P\frac{V_j^{k+1} - V_j^k}{\Delta t} = -g_{LP}\left(\frac{V_j^{k+1} + V_j^k}{2} - E_{LP}\right) + \frac{r_P}{2\rho_P}\left(D^+D^-\frac{V^{k+1} + V^k}{2}\right)_j \tag{16}$$

at the active and passive grid points respectively. D^+D^- is the second-order spatial centered finite difference operator

$$(D^+D^-\Phi)_j = \frac{\Phi_{j+1} - 2\Phi_j + \Phi_{j-1}}{\Delta x^2} \tag{17}$$

and the gating variables,g and E, are

$$g_j^{k+1/2} = \overline{g_{Na}}(m_j^{k+1/2})^3 h_j^{k+1/2} + \overline{g_K}(n_j^{k+1/2})^4 + \overline{g_L} \tag{18}$$

$$E_j^{k+1/2} = \frac{E_{Na}\overline{g_{Na}}(m_j^{k+1/2})^3 h_j^{k+1/2} + E_K\overline{g_K}(n_j^{k+1/2})^4 + E_L\overline{g_L}}{g_j^{k+1/2}} \tag{19}$$

We discretize the start and end boundary equations by taking a second-order Taylor expansion in space of the Hodgkin-Huxley equation, substituting for $\frac{\partial^2 V}{\partial x^2}$,solving for $\frac{\partial V}{\partial x}$ and substituting this value back into the boundary equation to find

$$i_0^{k+1/2} + \left(\frac{\pi r_A^2}{\rho_A}\right)\left(\frac{v_1^{k+1} + v_1^k - v_0^{k+1} - v_0^k}{2\Delta x}\right)$$
$$= r_A \Delta x_A \left(C_A \frac{V_0^{k+1} - V_0^k}{\Delta t} + g_1^{k+1/2}\left(\frac{V_0^{k+1} + V_0^k}{2} - E_1^{k+1/2}\right)\right)$$
$$\left(\frac{\pi r_A^2}{\rho_A}\right)\left(\frac{v_{n-2}^{k+1} + v_{n-2}^k - v_{n-1}^{k+1} - v_{n-1}^k}{2\Delta x}\right)$$
$$= r_A \Delta x_A \left(C_A \frac{V_{n-1}^{k+1} - V_{n-1}^k}{\Delta t} + g_1^{k+1/2}\left(\frac{V_{n-1}^{k+1} + V_{n-1}^k}{2} - E_1^{k+1/2}\right)\right)$$

We define the quantities associated with a junction between an active and passive cable

$$\widetilde{A_j} = \pi r_P \Delta x_P + \pi r_A \Delta x_A$$
$$\widetilde{g_j} = \frac{1}{\widetilde{A_j}}(r_P \Delta x_P g_P + r_A \Delta x_A g_A)$$
$$\widetilde{E_j} = \frac{1}{\widetilde{A_j}\widetilde{g_j}}(r_P \Delta x_P g_P E_P + r_A \Delta x_A g_A E_A)$$
$$D_A = \frac{\pi r_A^2}{2\Delta x_A \rho_A}$$
$$D_P = \frac{\pi r_P^2}{2\Delta x_P \rho_P}$$

where Δx_A and Δx_P represent the spatial grid sizes in the active and passive cables respectively. The variables g_A, g_P,E_A and E_P represent the g and E values in the discretized cable segments directly next to the junction in the active and passive cables respectively. With these defined, we discretization the junction with a Taylor expansion method similar to the one used in the start and end boundaries

$$\left(\frac{\widetilde{A_j}C}{\Delta t} + \frac{\widetilde{A_j}\widetilde{g_j}^{k+1/2}}{2} + D_P + D_A\right)V_j^{k+1} - D_P V_p^{k+1} - D_A V_A^{k+1} =$$
$$\left(\frac{\widetilde{A_j}C}{\Delta t} + \frac{\widetilde{A_j}\widetilde{g_j}^{k+1/2}}{2} - D_P - D_A\right)V_j^k + D_P V_P^k + D_A V_A^k \tag{20}$$

These equations result in a tridiagonal system

$$\begin{bmatrix} b_1 & c_1 & 0 & 0 & \dots & 0 \\ a_1 & b_2 & c_2 & 0 & \dots & 0 \\ 0 & a_2 & b_3 & c_3 & \dots & 0 \\ \vdots & \ddots & \ddots & \ddots & & \vdots \\ 0 & \dots & & 0 & a_{n-1} & b_n \end{bmatrix} \begin{bmatrix} \vdots \\ V_{j-1}^{k+1} \\ V_j^{k+1} \\ V_{j+1}^{k+1} \\ \vdots \end{bmatrix} = \begin{bmatrix} \vdots \\ d_{j-1}(V^k) \\ d_j(V^k) \\ d_{j+1}(V^k) \\ \vdots \end{bmatrix}$$

We solve this system using a linear time tridiagonal matrix solving algorithm which is stable in this case because our matrix is diagonally dominant. This method uses an average of V_k and V_{k+1} to implicitly solve for the next time step. The time step in the gating variables are evaluated at every half interval between the V_k steps so that $s^{k+1/2}$ can be calculated using V^k and V^{k+1} can be calculated using $s^{k+1/2}$. This leap frog scheme maintains the second order accuracy of the system in time while separating the calculations of the gating variables and voltage to avoid having to solve an implicit system in the voltage and gating variables together. We also use a centered finite difference scheme to ensure second order accuracy of the method in space. We thank Professor Charles Peskin for helping us with the equations and the discretization of the boundaries and junctions.

5 Results

We ran the simulation with a time step size of $\Delta t = 0.2\ \mu sec$, an active cable step of $\Delta x_A = 0.4\ \mu m$ and a passive cable step of $\Delta x_P = 2\ \mu m$. The total length of the cable was approximately 21 cm with 20 Nodes of Ranvier, 21 passive cable sections and 2 active sections on each end of the cable. The entire cable was discretized into 106,100 grid points.

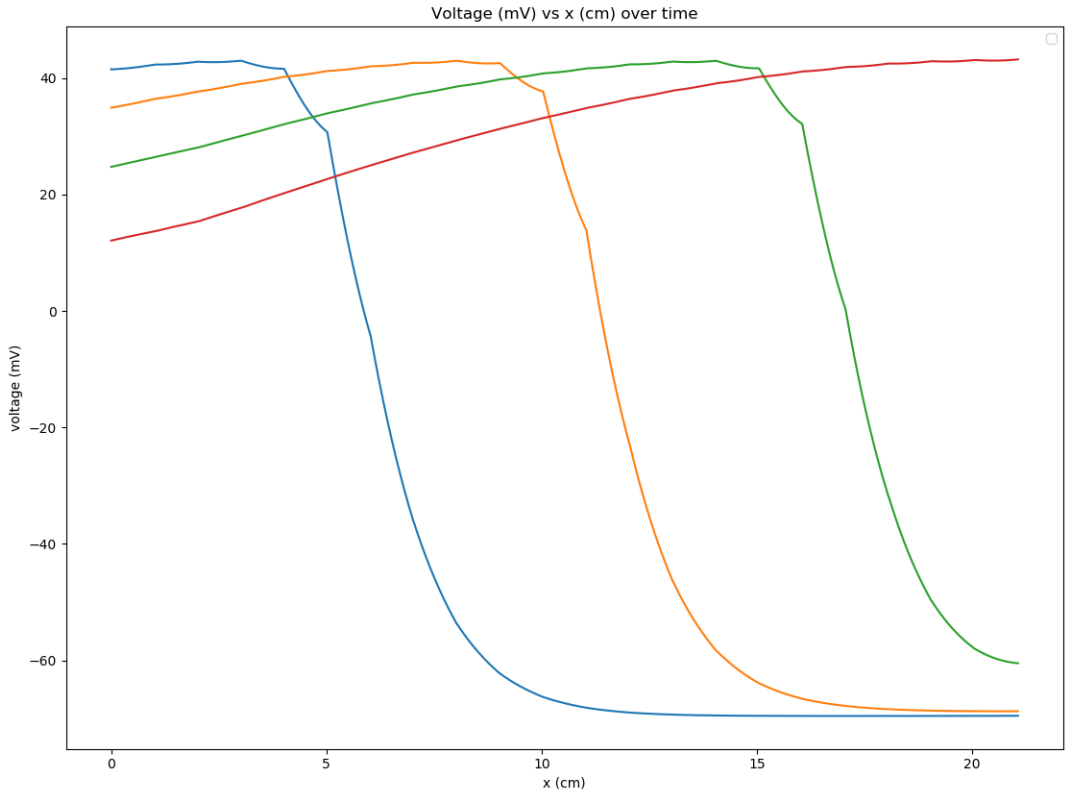

Figure 1: Action Potential at t = 0.4, 0.8, 1.2, and 1.6 msec

We found that the action potential generated in the myelinated axon propagates at a speed of approximately 100 m/s while the speed of the action potential in the unmyelinated axon propagates at a rate of 5 m/s. The length of the actual spike in the myelinated section is much longer because the wave propagates farther before the potassium ion channels can bring the voltage back down. We can see in Figure 1 that the action potential propagates across an entire 20 cm long cable in less than 2 msec. We can also see that the points with Nodes of Ranvier are not completely smooth, and there is a sudden change in voltage from one passive cable to the next. Animations for these action potentials as well as the code used to generate them can be found at `https://github.com/richard-xu1/Numerical-Methods-II-Project`.

In figure (2), we simulated the unmyelinated cable for 20 msecs and found that the voltage barely propagates 10cm in that time. However, it's clear that the spikes are much more concentrated and there is a clear hyperpolarization after the initial spike. Thus, our unmyelinated action potential travels at a speed of around

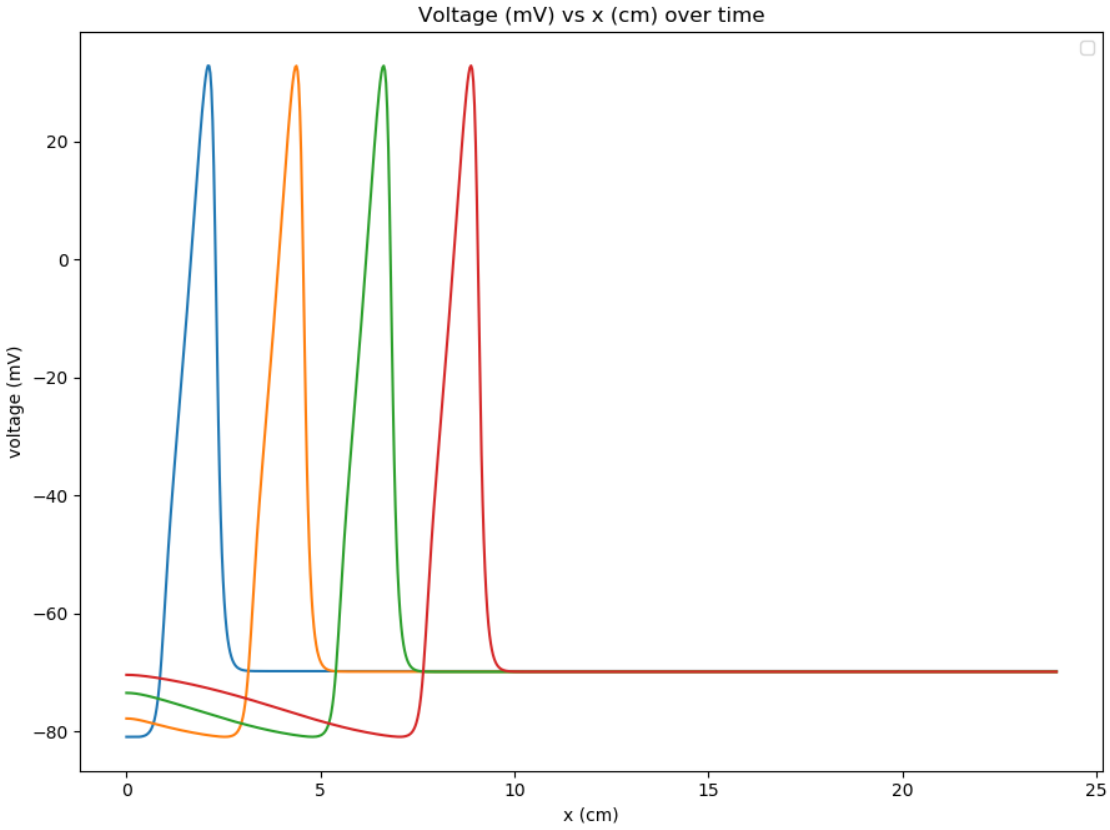

Figure 2: Action Potential at t = 4, 8, 12, and 16 msec

5m/s and our myelinated action potential traval at a speed of around 100 m/s. Since saltatory conduction is typically 10 to 30 times faster than normal conduction, our results are in the range of what they should be.

Figure (3) shows a few values we found in the myelinated case when running a convergence study in time by calculating

$$p = \log_2 \left(\frac{v_4 - v_2}{v_2 - v_1} \right)$$

where v_4 is the voltage using a time step $4dt$, v_2 is a voltage using $2dt$ and v_1 is a voltage using just dt. We checked around 200 values between 0.2 and 0.4 milliseconds, all of which were around 1.9 to 2.

Figure(4) shows a spatial convergence study on the unmyelinated cable on distances between 0.5 to 1 cm. We can see that the order of our convergence was again 2. Unfortunately, we were unable to achieve the same results for our myelinated case. When we tested our convergence order for a single passive cable between two Nodes of Ranvier, we lost one order of accuracy. We think this is likely because there is a bug in our code for calculating the voltage at the junctions. The method described above can be used for a tree of axons using appropriate numbering of nodes on the tree.

t	p
0.202	1.9899
0.222	1.9618
0.244	1.9291
0.270	1.9208
0.300	1.8991
0.314	1.8991
0.332	1.8911
0.390	1.8809

Figure 3: Convergence order of myelinated cable potential at time t in milliseconds

x	p
0.5	2.046
0.58	2.052
0.66	2.059
0.72	2.069
0.78	2.082
0.86	2.114
0.92	2.173
0.98	2.419

Figure 4: Convergence order of unmyelinated cable at distance x in cm

6 Conclusion

Overall, our results from comparing the myelinated and unmyelinated Hodgkin-Huxley model results are fairly consistent with experimental observations. Our method was second order accurate in time in the myelinated cable and second order accurate in both space and time in the unmyelinated cable. However, we were unable to accurately calculate the convergence in space in the myelinated version due to a problem with how we defined our junctions in the code.

It's important to note that are simulations do not perfectly replicate the physical properties of a myelinated cable because we used the Hodgkin and Huxley model as the basis for our model. The Hodgkin-Huxley equations used parameters that were based off a squid giant axon that behave very differently from a myelinated cable. Another factor we did not account for is that true myelinated fibers are extremely thin and the Nodes of Ranvier are typically only $1\mu m$ in length. Our Nodes of Ranvier, cable radius as well as internodal sections were both much larger than a typical myelinated axon. Because, we used parameters associated with a very large axon as the basis for our model, we weren't able to significantly decrease the size of the cable without affecting the results of our calculations.

It should also be noted that internodal sections are typically 1000 times longer than myelinated sections but ours is only 500 times longer. We were unable to make the voltage propagate through the entire cable with such a large passive cable. We believe this is likely because the properties of our cable is still too similar to that of a squid's axon, rather than a vertebrate's.

Finally, a typical myelinated axon does not experience hyperpolarization due to a much smaller potassium conductance, a larger sodium inactivation and more leakage in the active sections. Hyperpolarization in a myelinated axon would make the axon very slow in quickly propagating multiple action potentials. We did not try to account for this in our model so our myelinated axon due to the difficulty in converting the

parameters of the squid giant axon into the appropriate ones for replicating this behavior.